Proceedings of Global Power and Propulsion Society
ISSN-Nr: 2504-4400
GPPS Hong Kong 2023
October 17-19, 2023
www.gpps.global

GPPS-TC-2023-0204

Investigation on the influence of wavy leading edge on the noise and aerodynamic performance of an axial-flow fan

Liangji zhang
School of Power and Energy, Northwestern Polytechnical University
zhangliangji@mail.nwpu.edu.cn
Xi'an Shaanxi, P.R.China.

Hang Tong
School of Power and Energy, Northwestern Polytechnical University
tonghang@mail.nwpu.edu.cn
Xi'an Shaanxi, P.R.China.

Jianxin Lian
School of Power and Energy, Northwestern Polytechnical University
lianjianxin@mail.nwpu.edu.cn
Xi'an Shaanxi, P.R.China.

Weijie Chen
1.School of Power and Energy, Northwestern Polytechnical University；2.Collaborative Innovation Center for Advanced Aero-Engine
cwj@mail.nwpu.edu.cn
Xi'an Shaanxi, P.R.China.

Weiyang Qiao
School of Power and Energy, Northwestern Polytechnical University
qiaowy@nwpu.edu.cn
Xi'an Shaanxi, P.R.China.

ABSTRACT

A numerical simulation of the axial fan blade with wavy leading edge was carried out to study the influence on the performance and noise generation of the axial fan. Firstly, taking a single-stage axial fan as the research object, a method combined Delayed Detached Eddy Simulation (DDES) and the penetrable surface sound source integration method(AApsd) is used to calculate the flow field and sound field. During the study, it was found that after the amplitude of wavy leading edge stator exceeds 18mm, increasing the amplitude would not significantly improve the noise reduction. Further study found that the wavy leading edge stator configuration could effectively reduce the amplitude and correlation of unsteady load on the leading edge of the stator. However, the wavy leading edge stator causes additional noise source near the suction plane trough, and its intensity is closely related to the amplitude of the wavy leading edge stator. Finally, the mechanization of additional noise sources is explained.

INTRODUCTION

With the rapid development of the world economy and the international commercial air transport industry, the noise pollution of commercial aircraft has attracted more and more attention (Enghardt, 2019).

For aircraft noise, engine noise occupies a dominant position(Owens, 1979). In the past few decades, thanks to the use of high bypass ratio commercial aircraft engines, the nozzle exit velocity has been significantly reduced, and the engine jet noise has been effectively controlled. However, the increase of the engine bypass ratio will increase the size of the fan, the fan tip speed will also increase, and the fan noise will become another significant noise source(Hughes, 2013).

Fan noise can be divided into two categories : fan rotator / stator interference single-tone noise (Wang ,2017, Tong et al. 2020, Tong et al.,2021) and fan broadband noise (Tong et al., 2018, Polacsek et al., 2015, Tong et al., 2021). With the development of computer technology, the prediction method of the single-tone noise and single-tone noise control technology have developed maturely. Due to the complexity of fan turbulence broadband noise, the prediction method and control technology of fan turbulence broadband noise have been developing slowly. Along with the effective control of fan rotator / stator interference single-tone noise (Edmane, 2002), the engineering problem of fan broadband noise has become a major problem that modern civil aviation has to face (Yan et al.,2022).

For the prediction of fan broadband noise, using CFD to accurately simulate the rotor wake turbulence and stator interference process requires Delayed Detached Eddy Simulation (DDES)(Chen et al., 2023) and Large Eddy Simulation (LES) (Shi et al., 2023). LES method needs a lot of computing resources to simulate the fan flow field, which is costly and lacks timeliness. It is still not suitable for industrial design and large-scale calculation. As a hybrid method of URANS and LES, DES can significantly reduce the number of grids while ensuring the calculation accuracy, thereby reducing the calculation cost. In recent years, the improved model DDES method of DES has been applied in industry (Michael, 2019), and some scholars have begun to apply it to noise calculation (Takao, 2018, Benjamin,2021).

Many scholars have applied wavy leading edge technology to aircraft wings (Chaitanya, 2017), and found that it has many advantages such as improving stall and reducing turbulent broadband noise. In recent years, some scholars have applied wavy leading edge technology to turbomachinery (Feinerman et al., 2017, Damiano et al., 2019, Zhu et al., 2022). However, due to the complexity of internal flow, the application of wavy leading edge technology in turbomachinery is not very mature. There are still a lot of problems and theories to be studied and explained. It is necessary to further study the influence of wavy leading edge blades on the aerodynamic performance and noise of turbomachinery.

In this paper, the fan noise calculation method based on the penetrable surface method is used to study the influence of wavy leading edge configuration technology on the aerodynamic performance and noise of a single-stage axial flow fan.

METHODOLOGY

In this paper, the calculation method of fan noise based on Acoustics Analogy (AA) theory is adopted.The calculation formula of sound power ζ_{mn} in fan duct is(Wang, 2017, Tong et al., 2020)：

$$\zeta_{mn}(\omega) = \frac{\pi(r_D^2 - r_H^2)}{\rho U} \cdot \frac{\mp Ma^2(1-Ma^2)^2(\omega/U)k_{mn}(\omega)}{[\omega/c \pm Mak_{mn}(\omega)]^2} \cdot [A_{mn}(\omega)\cdot(A_{mn}(\omega))^*] \quad (1)$$

Where, m and n are the circumferential mode order and the radial mode order of the annular duct ; ω is the angular frequency ; r_D and r_H is the casing radius and the hub radius ; ρ is the gas density ; U is the airflow velocity ; Ma is the Mach number ; c is the sound velocity ; k is the axial wavy number ; and A_{mn} is the amplitude of the acoustic mode at specific frequency and mode (m,n) :

$$A_{mn}(\omega) = \frac{\mathrm{i}}{2\pi(r_D^2 - r_H^2)\kappa_{mn}} \cdot \int_{S_F} \{\Psi_m(\kappa_{mn} r)\cdot \vec{n} \cdot \nabla[\exp(-im\theta + ik_{mn}x)] L_{ij}\} ds \quad (2)$$

Where, Ψ_{mn} and κ_{mn} are the modal characteristic function and eigenvalue of the annular duct; x,r,θ are the axial, radial and circumferential coordinates in the cylindrical coordinate system; S_F is the sound source surface. $\vec{n}$ is the outer normal vector of the sound source surface; L_{ij} is the stress tensor. Subscripts i and j are the Wall normal vector and the direction of the wall force:

$$L_{ij} = [\rho u_i(u_j + U_{0j} - v_j) + P_{ij}] \quad (3)$$

$$P_{ij} = (p - p_0)\delta_{ij} - \sigma_{ij} \quad (4)$$

$$\sigma_{ij} = \mu\left(\frac{\partial u_i}{\partial x_j} + \frac{\partial u_j}{\partial x_i} - \frac{2}{3}\frac{\partial u_k}{\partial x_k}\delta_{ij}\right) \quad (5)$$

Where, subscripts 0 represents the environmental variable, u represents the instantaneous fluid velocity, A represents the instantaneous limiting streamline velocity, δ_{ij} is the unit tensor, and μ is the viscosity coefficient of the fluid.

For the rotor / stator interference single-tone noise, the sound power can be obtained by superimposing the dominant modal sound power of formula (equation 1). For broadband noise, it is necessary to superimpose all the modal sound power which is taking on.

MODEL AND NUMERICAL SET UP

Model

The Aero-acoustic synthesis of single-stage axial fan in Northwestern Polytechnical University(NPU-Fan) is simulated in this paper, and the schematic diagram and design parameters of NPU-Fan are given in Figure 1 and Table 1. The NPU-Fan is mainly composed of an inlet section, an acoustic measurement section, a test section, and a muffler exhaust duct. A manual throttling cone is installed at the rear of the exhaust duct to control the working flow. The fan is powered by an 18.5 kW motor. In order to improve the accuracy of noise measurement, the inlet section of NPU-Fan is installed in a semi-anechoic chamber.

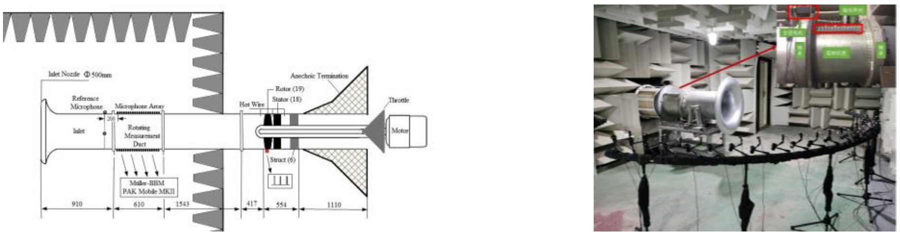

(a) Schematic diagram of the NPU-Fan structure (b) Photo of the NPU-Fan

Figure 1 Diagram of NPU-Fan

Table 1 NPU-Fan design parameter

Parameter	Value
Rotor blade number	19
Stator blade number	18
Shroud diameter（m）	0.5
Hub diameter（m）	0.285
Massflow（kg/s）	6.38
Design speed（r/min）	3000
Total pressure ratio	1.02
Airfoil shape	NACA-65

Numerical set up

To improve computational efficiency, the NPU-Fan is domain scaled before the broadband noise calculation. Reduce the numberof blades from 19 to 18. Ensure that the reduced rotor blade consistency is consistent with the original rotor blade consistency by increasing the rotor blade size.

Figure 2 shows the comparison results of the aerodynamic performance of the reduced fan and the original fan. It can be seen that after the number of rotor blades is reduced from 19 to 18, the total pressure ratio characteristics and efficiency characteristics of the two are basically consistent.

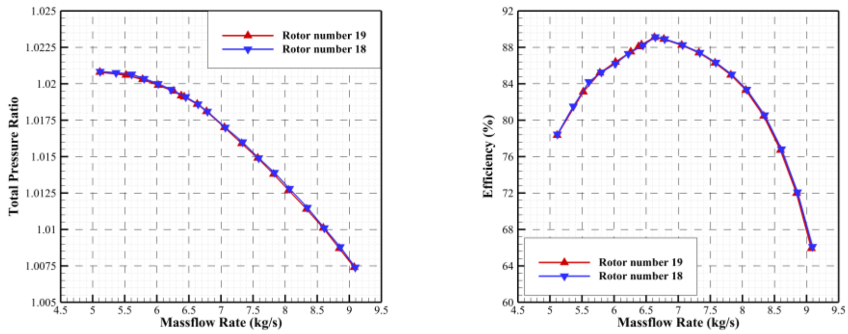

(a) Total pressure ratio (b) Efficiency

Figure 2 Effect of reduced rotor blade numbers on aerodynamic performance

Figure 3 is a schematic diagram of the unsteady calculation domain structure of a single-stage fan. The total grid number of rotor domain is about 1.951 million, There are 45 grid points in blade tip clearance, and 301 grid points in spanwise direction. The first grid thickness neart he wall grid is 0.003 mm. Over most of the blade surface, The dimensionless mesh scale $\Delta x^+ < 250$， $\Delta y^+ < 1$， $\Delta z^+ < 150$.

The leading edge of stator blade is the main source of noise, so its mesh is denser. The total grid number of stator domain is about 1.515 million, There are 381 grid points in spanwise direction. The first grid thickness neart he wall grid is 0.003 mm. Over most of the blade surface, The dimensionless mesh scale $\Delta x^+ < 200$， $\Delta y^+ < 1$， $\Delta z^+ < 75$.

The inlet boundary condition of the calculation domain is the total pressure boundary condition : 97700 Pa, the outlet is the average static pressure boundary condition, the solid wall is the non-slip boundary condition, and the circumferential rotation period boundary condition is used. In the calculation, the governing equation is solved by the finite volume method, the spatial discretization scheme is the second-order difference scheme, the time difference scheme is the second-order backward Euler difference scheme, and the turbulence model is the DDES (Delayed-Detached-Eddy-Simulation) turbulence model. The unsteady calculation takes the steady calculation results as the initial conditions, and the rotor single channel is divided into 50,100， 150($\Delta t = 7.407 \times 10^{-6}$) time steps to advance three rotation cycles. The flow field information of 13500 time steps in 5 rotation cycles was counted. The penetrating surface of the acoustic calculation is Plane 1 and Plane 1 in Figure 3(b).

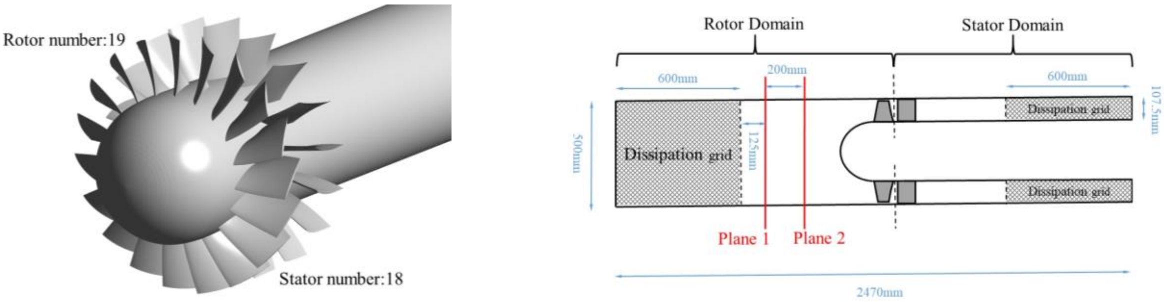

(a) Diagram of CFD computational domain (b) Size of CFD computational domain

Figure 3 Diagram of NPU-Fan unsteady computational domain

In this paper, the influence of three amplitude wavy leading edge blades on fan broadband noise is studied.The definition of the wavy leading edge blade is detailed in References (Tong et al., 2020), where A represents the amplitude, W represents the wavylength, and the unit is mm.Figure 4 shows the diagram of wavy leading edge stator blades.

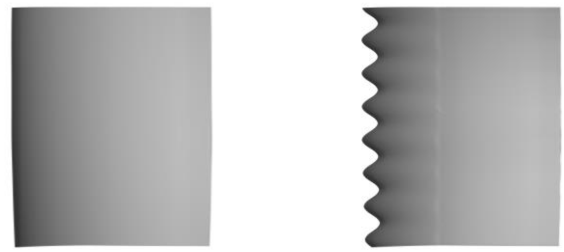

(a) baseline (b) A9W15

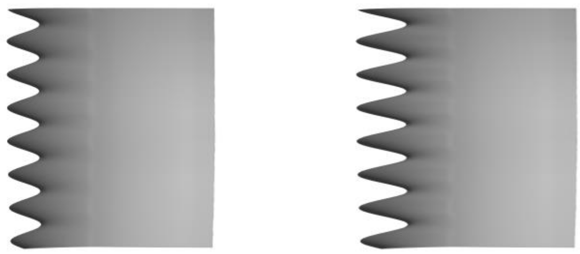

(c) A18W15 (d) A27W15

Figure 4 Diagram of wavy leading edge stator blade of NPU-Fan

Verification of calculation method

In order to verify the correctness of the numerical simulation method, NPU-Fan is used as the test object. Figure 5 shows the comparison between the AA method using the blade surface as the sound source (Wang, 2017), the AApds method with Plane1 as the integral surface and the experimental results. It can be seen that because the AA method does not take into account the shielding effect and scattering effect of the rotor blade on the sound wavy, the results of the AA method are obviously larger, and the results obtained by the AApds method are less than 3dB compared with the experimental results. In general, the fan noise calculation method based on the penetrable surface method used in this paper is accurate.

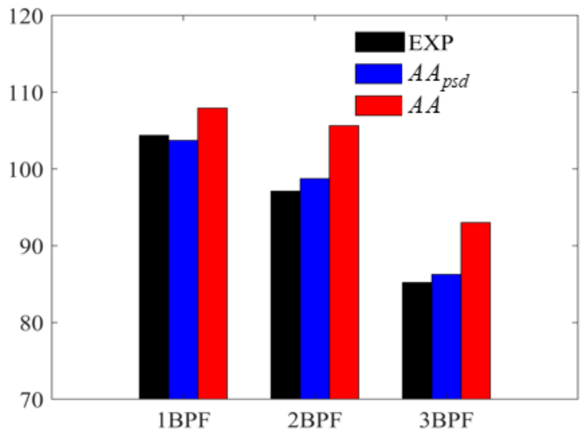

Figure 5 Comparison of results of NPU-Fan rotor/stator interaction tonal noise

RESULTS AND DISCUSSION

Aerodynamic results

Figure 6 shows the influence of wavy leading edge of fan stator vane on the aerodynamic performance of the single-stage fan. From Figure 6 (b), it can be seen that with the increase of the amplitude of the leading edge vane, the peak efficiency and design point efficiency of the fan gradually decrease, which shows that the increase of the amplitude of the leading edge vane is not conducive to the performance of the design point of the fan. The reason is that the wavy leading edge will cause additional leading edge loss at the design point. In addition, it can be seen from Figure 6 that the wavy leading edge guide vane obviously broadens the working range of the fan and improves the flow state of the leading edge under small flow conditions.

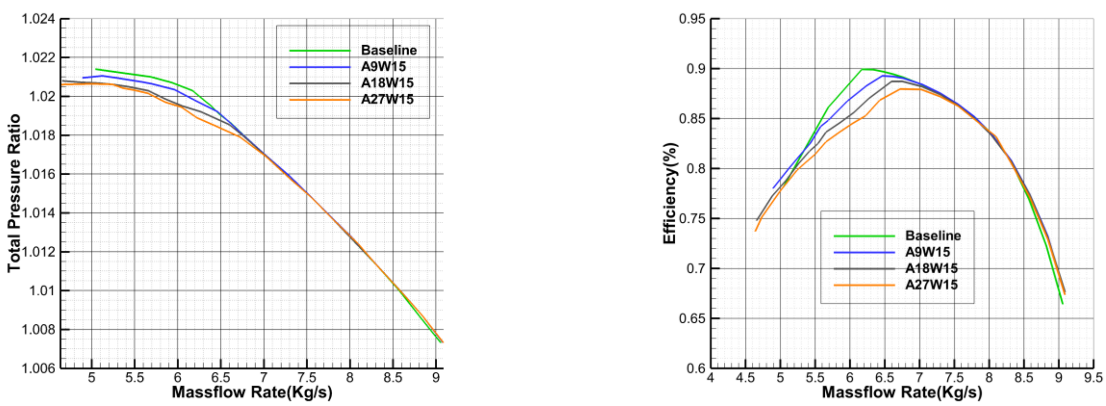

(a) Total pressure ratio

(b) Efficiency

Figure 6 Effect of compositing type blade configuration on aerodynamic performance

Aeroacoustic results

Fig.20 shows the single-tone noise prediction results of different wavy leading edge vanes under design conditions. After using the wavy leading edge vanes, the single-tone noise level of rotor / stator interference is reduced, which basically meets the trend that the greater the amplitude, the better the noise reduction effect.

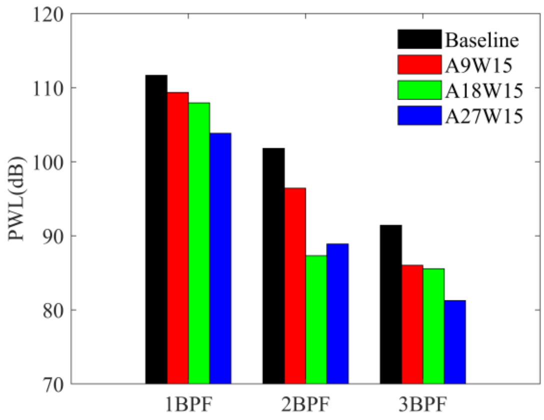

Figure 7 Prediction results of tonal noise

Figure 8 show the broadband noise prediction results of different configurations of stator vanes. It can be seen from the figure that the wavy leading edge vanes with different amplitudes can reduce the fan broadband noise. The noise reduction of A18W15 and A27W15 is better than that of A9W15. However, A27W15 cannot further improve the noise reduction compare with A18W15. Therefore, the broadband noise can be reduced by the wavy leading edge configuration, but the amplitude also has a critical value. When it is greater than this critical value, the broadband noise cannot be further reduced.

In addition, it can be seen from the diagram that the initial noise reduction frequencies of A9W15 and A18W15 blades are about 3kHz and 1.5kHz, respectively. Under the design condition, the average velocity of the stator inflow is about 50m / s. According to the empirical formula(equation 6) of Reference Narayanan, 2014,the two kinds of wavy leading edge blades basically meet the law of Reference Narayanan, 2014.

$$f = \alpha U / A, \quad \alpha \approx 0.5 \tag{6}$$

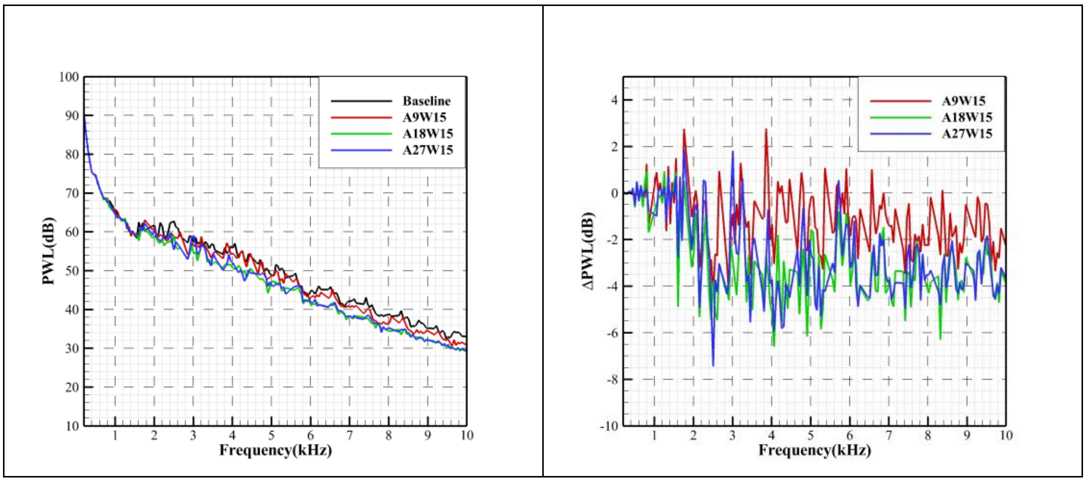

Figure 8 Prediction results of broadband noise

Noise reduction mechanisms

Figure 9 shows the unsteady load distribution of stator vanes under design conditions. From the figure, it can be seen that the main sound source is located at the leading edge of the stator blade. After using the wavy leading edge, the unsteady load distribution on the blade surface has changed significantly. On the one hand, the unsteady load intensity on the blade pressure surface has been weakened to a certain extent. On the other hand, the position of the main sound source has also changed significantly. The position near the trough of the suction surface becomes the strongest sound source, while the unsteady load level at the peak and the hill position is significantly reduced, and the strength of the main sound source tends to increase with the increase of the amplitude.

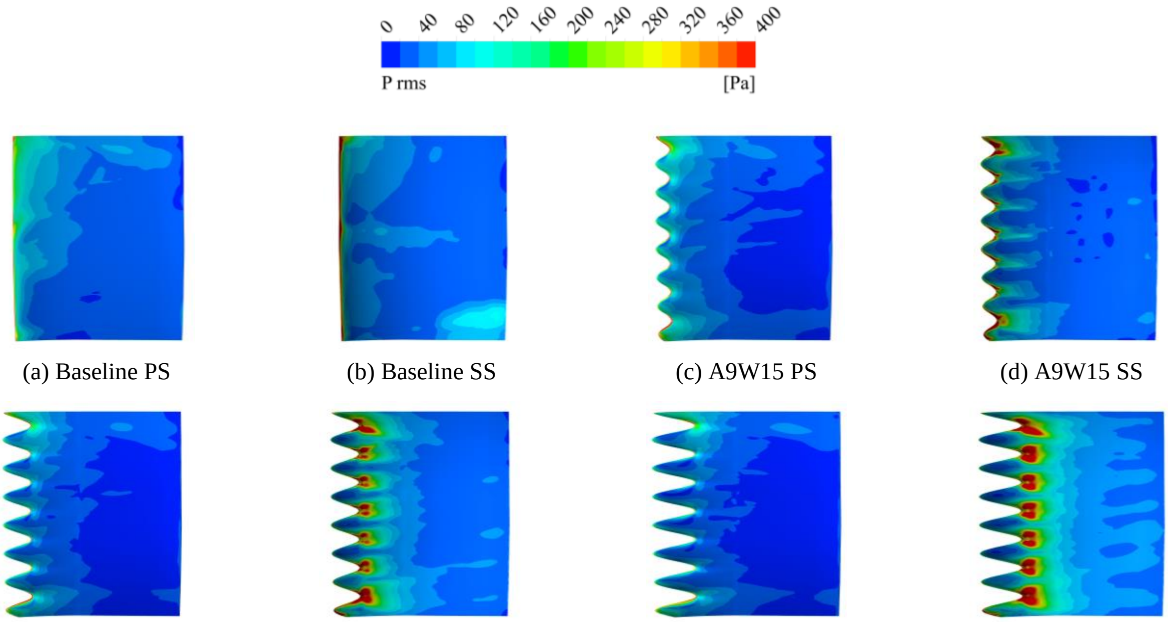

(a) Baseline PS (b) Baseline SS (c) A9W15 PS (d) A9W15 SS

(e)A18W15 PS (f)A18W15 SS (g)A27W15 PS (h)A27W15 SS

Figure 9 Contour of unsteady load distribution on stator blade surface

Figure 10 shows the flow field structure of A18W15 blade. From Figure 10 (a), it can be seen that the interference structure of counter-rotating vortex appears in the trough area of A18W15 blade, and the counter-rotating vortex gradually develops into a hairpin vortex structure with the mainstream flow after interference. The schematic diagram of the formation of the counter-rotating vortex structure is given in Figure 10 (b). Since the peak of the stator pressure surface is in the high pressure region and the trough is in the low pressure region, the secondary flow from the peak to the trough is the main power source for the migration and interference of the counter-rotating vortex.

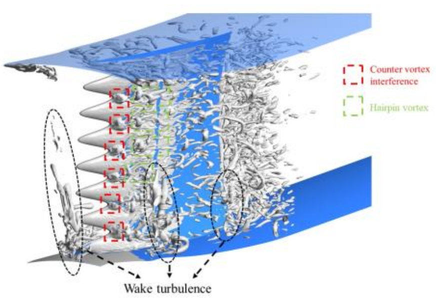

(a) Transient vortex structure(Q=1.4×10^{-7} s^{-2})

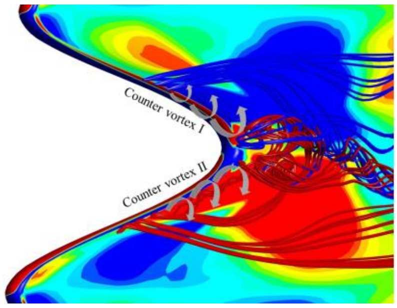

(b) Three-dimensional streamline structure

Figure 10 Flow field structure of A18W15 stator

Figure 11 shows the flow structure diagram of the wavy leading edge. It can be seen from Figure 11 (a) that the suction surface and the pressure surface of the blade will generate two reverse radial vortices. Under the action of the incoming vortex, the radial vortex of the suction surface will be enhanced, while the radial vortex of the pressure surface will be weakened. Therefore, the enhanced radial vortex of the suction surface will increase the upwash velocity of the suction surface, and the unsteady load strength of the suction surface will be enhanced after the upwash velocity and the suction surface act. It can be seen from Figure 11 (b) that the counter-rotating vortex is enhanced under the action of the incoming vortex and the pressure difference between the pressure surface and the suction surface.

Figure 11(c) gives the flow topology of the wavy leading edge blade, combined with Figure 11(a), the flow of the wavy leading edge blade can be divided into three steps : 1.When the airflow meets the peak, the horseshoe vortex structure is generated at the peak ;2. The two horseshoe vortex branches of the adjacent peaks develop along the mainstream, which are enhanced by the inflow vortex and the pressure difference between the pressure surface and the suction surface, and further meet and interfere behind the trough, resulting in a strong noise source ;3. The counter-rotating vortex after interference continues to develop with the mainstream and finally generates the hairpin vortex structure.

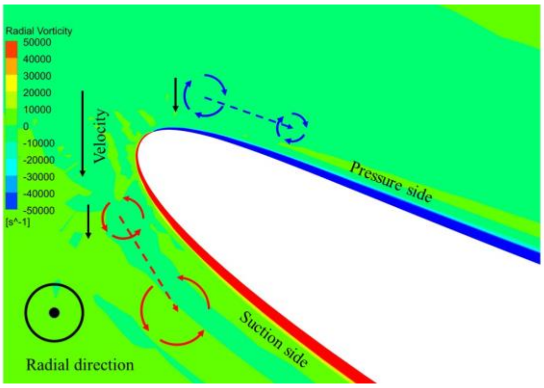

(a) Contour of radial vorticity distribution at radial section

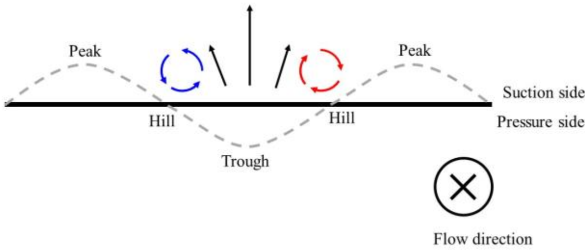

(b) Counter vortex flow structure at wavy leading edge

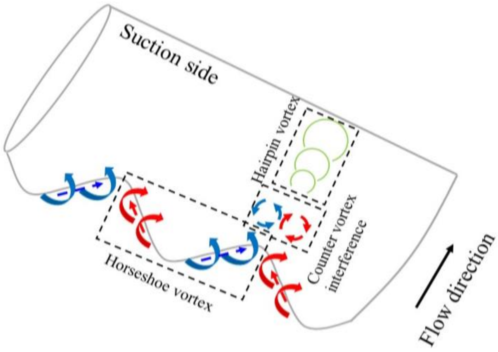

(c) Flow topology of wavy leading edge blade

Figure 11 Flow structure schematic diagram of wavy leading edge blade

CONCLUSIONS

The noise of NPU-Fan is calculated by DDES method combined with the fan noise calculation method based on the acoustic analogy theory of penetrable surface. The results show that the wavy leading edge configuration reduces the aerodynamic performance of the design point, but can broaden the stable operating range of the fan. The wavy leading edge stator blade can reduce the fan single tone and broadband noise. It is found that blindly increasing the amplitude cannot further improve the noise reduction effect. And the initial noise reduction frequency basically meets this rule.

In this paper, the noise reduction principle of stator blades with wavy leading edge configuration is deeply studied. The main noise source of turbulence / blade interference is concentrated on the leading edge of the blade, so the wavy leading edge blade can obviously weaken the unsteady load of the blade leading edge, that is to say, the wavy leading edge blade can effectively reduce the turbulence / blade interference noise. However, the wavy leading edge blade will introduce additional noise sources, which are mainly located near the rear of the trough.

ACKNOWLEDGMENTS

This study is co-supported by the National Science and Technology Major Project of China (No. 2017-Ⅱ-0008-0022), the National Natural Science Foundation of China (Nos.52276038, 51936010, 51776174 and 52106056), the Fundamental Research Funds for the Central Universities (No. 3102021OQD706), and the National Key Laboratory of Science and Technology on Aerodynamic Design and Research (No. 614220121050103). the Science Center for Gas Turbine Project (No. P2022-A-II-003-001, P2022-B-II-011-001), the Fundamental Research Funds for the Central Universities (No. 3102021OQD706, 501XTCX2023146001), the National Key Laboratory of Science and Technology on Aerodynamic Design and Research (No. 614220121050103), and the Laboratory of Aerodynamic Noise Control (No. ANCL20210104, ANCL20220101).

REFERENCES

Enghardt L.(2019). Aeroacoustics research in Europe: The CEAS-ASC report on 2017 highlights. Journal of Sound and Vibration,, 450,pp.175-198.

Owens R.(1979). Energy efficient engine: Propulsion system - aircraft integration evaluation. Technical Report, NASA/CR 159488.

Hughes C.(2013). NASA collaborative research on the ultra high bypass engine cycle and potential benefits for noise, performance, and emissions. Technical Report, NASA Technical Memorandum TM-2013-216345.

Wang L F.(2017). *Experiment and numerical study on duct mode identification of fan noise*. Northwestern Polytechnical University.

Tong H, Li L, Mao L Q , et al(2020). Tonal noise reduction of a high-speed single axial fan with wavy leading-edge stator. *Acta Aeronautica et Astronautica Sinica*, 41(10),pp.123565.

Tong H, Ding S, Xiang X S , et al.(2021). Numerical study on tonal noise reduction of single axial fan with distributed wavy leading-edge stator. *Journal of Propulsion Technology*, , 42(10),pp. 2237-2248.

Tong F, Qiao W Y, Xu K B, et al.(2018). On the study of wavy leading-edge vanes to achieve low fan interaction noise. *Journal of Sound and Vibration*, 419,pp. 200-226.

Polacsek C, Clair V, Le G, et al.(2015). Numerical predictions of turbulence/cascade-interaction noise usingcomputationalaeroacoustics with a stochastic model. *AIAA Journal*, 53,pp.3551-3566.

Tong H, Li L, Wang L F, et al.(2021). Investigation of rotor–stator interaction broadband noise using a RANS-informed analytical method. *Chinese Journal of Aeronautics*,, 34(10): 53-66.

Edmane E.(2002). Fan noise reduction: an overview. *Aeroacoustics*, 1(1),pp.43-64.

Yan Q, Xue D W, Gao X, et al.(2022). Acoustic performance experimental technology of aircraft nacelle acoustic liner. *Acta Aeronautica et Astronautica Sinica*, 43(6),pp. 526810.

Chen H,Yuan X X, Bi L, et al.(2023). Simulation of separated flow based on RANS/LES hybrid method. *Acta Aeronautica et Astronautica Sinica*, 44(2),pp.626310.

Shi F C,Gao Z X, Tian Y Y, et al.(2023). Large eddy simulation of ideally expanded supersonic jet noise. *Acta Aeronautica et Astronautica Sinica*, 44(2),pp.626266..

Michael S, Michael S, Andrey T.(2018). Unsteady Simulations of a Fan/Outlet-Guide-Vane System: Aerodynamics and Turbulence. *AIAA Journal*,, 56(6), pp.2283-2297.

Takao S, Philippe R S, Michael L S. et al.(2018). Unsteady simulations of a fan/outlet-guide-vane system: tone–noise computation. *AIAA Journal*, 56(6), pp. 3558-3569.

Benjamin F, Raphael B.(2020). *Zonal detached eddy simulation of the fan-OGV stage of a modern turbofan engine*. ASME Turbo Expo 2020, GT 2020-14239, 2020.

Chaitanya P, Joseph P, Narayanan S, C, et al.(2017). Performance and mechanism of sinusoidal leading edge serrations for the reduction of turbulence–aerofoil interaction noise. *Journal of Fluid Mechanics*, 818, pp.435-464.

Feinerman J A, Koushik S, Schmitz F H.(2017). Effect of leading-edge serrations on helicopter blade–vortex interaction noise. *Journal of the American Helicopter Society*, 62,pp. 1-11.

Damiano C., Francesco A., Ignacio G .M., et al..(2019) Aeroacoustic study of a wavy stator leading edge in a realistic fan/OGV stage. *Journal of Sound and Vibration*,pp.138-154.

Zhu X Y., Guo Z P., Zhang Y F, et al..(2022) Numerical study of aerodynamic characteristics on a straight-bladed vertical axis wind turbine with bionic blades. *Energy*, pp.122453

Narayanan, S., Joseph, P., Haeri, S., Kim, J.W. (2014). Chaitanya, P., Polacsek, C. Noise Reduction Studies from the Leading Edge of Serrated Flat Plates.. Atlanta, GA: AIAA.